BRAIN CONNECTIVITY
Volume 4, Number 9, 2014

DOI: 10.1089/brain.2014.0286

# Age-Related Reorganizational Changes in Modularity and Functional Connectivity of Human Brain Networks

Jie Song,[1,2] Rasmus M. Birn,[3,4] Mélanie Boly,[3,5] Timothy B. Meier,[1,6,7] Veena A. Nair,[1] Mary E. Meyerand,[1,2,4,6] and Vivek Prabhakaran[1,3–6,8,9]

## Abstract

The human brain undergoes both morphological and functional modifications across the human lifespan. It is important to understand the aspects of brain reorganization that are critical in normal aging. To address this question, one approach is to investigate age-related topological changes of the brain. In this study, we developed a brain network model using graph theory methods applied to the resting-state functional magnetic resonance imaging data acquired from two groups of normal healthy adults classified by age. We found that brain functional networks demonstrated modular organization in both groups with modularity decreased with aging, suggesting less distinct functional divisions across whole brain networks. Local efficiency was also decreased with aging but not with global efficiency. Besides these brain-wide observations, we also observed consistent alterations of network properties at the regional level in the elderly, particularly in two major functional networks—the default mode network (DMN) and the sensorimotor network. Specifically, we found that measures of regional strength, local and global efficiency of functional connectivity were increased in the sensorimotor network while decreased in the DMN with aging. These results indicate that global reorganization of brain functional networks may reflect overall topological changes with aging and that aging likely alters individual brain networks differently depending on the functional properties. Moreover, these findings highly correspond to the observation of decline in cognitive functions but maintenance of primary information processing in normal healthy aging, implying an underlying compensation mechanism evolving with aging to support higher-level cognitive functioning.

**Key words:** aging; brain networks; default mode network; efficiency; graph theory; modularity; resting-state functional connectivity; sensorimotor network

## Introduction

The topological aspects of human brain functional networks have drawn much attention in recent years. By modeling a large-scale brain network as a graph consisting of nodes (i.e., cortical and subcortical brain regions) and links (i.e., functional or anatomical connections among brain regions) (Rubinov and Sporns, 2010), it is possible to construct a systematic, topological examination of brain functional or anatomical organization. This concept highlights the idea of understanding the complex brain system from information about how individual voxels or brain regions interact via functional or structural connections. Furthermore, rather than ascribing significant group differences or effects to particular voxels, as is historically done in functional neuroimaging, this concept also helps us better understand how the brain network as a whole is organized in different populations.

Graph-theory-based complex network analysis approach provides a powerful way of understanding the dynamic interactions of different brain regions and how these interactions produce complex behaviors. Graph metrics such as modularity, local efficiency, global efficiency, and strength measures are often used to characterize brain network properties, especially for group comparison. Modularity, in particular, is a ubiquitous property of complex, large-scale functional brain networks. Modules consist of densely intraconnected brain regions that are sparsely inter-connected with regions in other modules (Newman and Girvan, 2004). Modular organization may represent stable subcomponents of the brain that facilitate the construction of a complex system from simple building blocks, and can be theoretically linked to network development

Departments of [1]Radiology, [2]Biomedical Engineering, [3]Psychiatry, [4]Medical Physics, and [5]Neurology, University of Wisconsin-Madison, Madison, Wisconsin.
[6]Neuroscience Training Program, University of Wisconsin-Madison, Madison, Wisconsin.
[7]Laureate Institute for Brain Research, Tulsa, Oklahoma.
[8]Medical Scientist Training Program and [9]Department of Psychology, University of Wisconsin-Madison, Madison, Wisconsin.

(Alexander-Bloch et al., 2010), which has provided insights into abnormal brain development, neuropsychological conditions (Alexander-Bloch et al., 2014; Peng et al., 2014; Xu et al., 2013), and age-related neurodegenerative diseases (Gottlich et al., 2013; Kikuchi et al., 2013). Therefore, in this study, we hypothesize that the brain functional modular structure can be affected by aging and that age-related changes in modularity can be revealed by graph theory analysis.

Previous studies on human brain aging have shown shrinkage of the adult brain as it ages, with a reported nonuniform pattern of changes in gray and white matter (WM) (Raz et al., 2005). These structural changes provide a fundamental basis for the hypothesized functional brain reorganization in relation to normal aging. Furthermore, previous graph theoretical analysis showed a substantial correspondence between structural connectivity and resting-state functional connectivity (RSFC) measured in the same subjects based on functional magnetic resonance imaging (fMRI) and diffusion spectrum imaging data (Hagmann et al., 2008). Here, we test the hypothesis that the normal modular structure of functional brain networks might be altered with aging along with potential changes in functional connectivity measures such as local efficiency, global efficiency, and strength. We further assessed these metrics at the local regional level for group comparison, which provides a finer-grained analysis of changes in network properties associated with aging.

## Materials and Methods

### *Data acquisition*

Participants were 26 younger adults (age 24.6 ± 3.3 years, 11 women) and 24 older adults (age 58.0 ± 6.1 years, 12 women) with no history of neurological or psychological disorders. Ten-minute resting-state fMRI scans were acquired from each subject as they rested with their eyes fixated on a cross projected to the center of a MR-safe screen. Imaging data were obtained on a 3.0 Tesla whole-body MRI scanner (DISCOVERY MR750; General Electric Medical Systems, Waukesha, WI) with an 8-channel receive-only RF head coil array. This study was approved by the University of Wisconsin-Madison Health Sciences Institutional Review Board. Written informed consent was provided by each participant.

T1-weighted structural images with 1 mm isotropic voxels were acquired axially with an MPRAGE sequence (TR = 8.132 ms, TE = 3.18 ms, TI = 450 ms, flip angle = 12°, field of view = 256 × 256 $mm^2$, matrix size = 256 × 256, slice thickness = 1 mm, and number of slices = 156). Echo planar imaging data were collected in the sagittal plane with the following parameters: TR = 2.6 sec, TE = 22 ms, flip angle = 60°, field of view = 224 × 224 $mm^2$, matrix size = 64 × 64, slice thickness = 3.5 mm, number of slices = 40 slices, and 231 volumes.

### *Data processing*

Resting-state fMRI data were processed in AFNI (Cox, 1996), including the following initial preprocessing steps: (1) despiking to remove extreme outliers in the signal intensity time courses, (2) correcting for motion and slice timing, and (3) removing first three time points of the scan (total 231 time points). T1-weighted structural images were warped to standard MNI space using a 12-parameter affine transformation. This transformation was combined with the T1-to-EPI alignment and used to map the functional EPI scans to MNI space with a resampling of 3 mm resolution. The resulting structural images were later skull stripped and segmented into gray matter, WM, and cerebrospinal fluid (CSF) masks using FSL (Smith et al., 2004). The average signal time course from the WM and CSF masks and the six rigid body motion parameters were normalized and regressed out. The residuals from the functional data were spatially smoothed with a 4 $mm^2$ full-width half maximum isotropic Gaussian kernel in AFNI and then temporally filtered with a band-pass from 0.01 to 0.1 Hz.

Head motion has been shown to significantly affect the RSFC measures (Saad et al., 2009; Satterthwaite et al., 2012; Van Dijk et al., 2012). Therefore, a secondary motion correction was performed to exclude certain time frames with motion above a more stringent threshold. A score of motion measurement corresponding to each time frame of fMRI scan was calculated as the square root of the sum of squares of the derivatives (SSD) of the six time courses of the motion parameters (Birn et al., 2013; Jones et al., 2010; Meier et al., 2012). In this study, any time frame associated with a score of SSD greater than 0.2 mm was censored and later excluded using the censor option provided in the AFNI program, 3dDeconvolve. This option essentially performed zero-filling to maintain the same sampling rate and the same length of time series for each subject. To further eliminate group differences in motion contaminating functional connectivity assessments, we matched subjects from the two age groups with their average motion SSD across all these time points. This process resulted in two subgroups with 16 subjects in each subgroup. Several younger subjects with small average motion SSD and several older subjects with relatively greater average motion SSD had to be removed in order to match the average motion for the two subgroups. The younger subgroup had an average motion SSD of 0.055 ± 0.018 mm, and the older subgroup had an average motion SSD of 0.058 ± 0.019 mm. There was no significant group difference in terms of the average motion SSD (two-sample t-test, $p$-values = 0.39). The younger subgroup (ages 24.6 ± 3.5 years, five women) and older subgroup (ages 56.5 ± 5.3 years, eight women) showed significant age differences (two-sample t-test, $p$-value < 0.00001), but no significant differences in gender (the chi-square test, $p$-value = 0.47). Our findings presented here were based on data from these two subgroups.

### *Resting-state functional connectivity*

The RSFC was computed from 187 different brain regions defined within the sensorimotor, cingulo-opercular task control, fronto-parietal task control, dorsal/ventral attention, default mode network (DMN), salience network and subcortical/cerebellar network (Power et al., 2011). In each of these brain regions, signals resulting from the processed functional data were extracted and averaged over a spherical region of interest (ROI) with a radius of 4 mm. Pearson correlation coefficient ($r_{ij}$) was calculated for the $i$th and $j$th ROI. This generated a 187 × 187 adjacency matrix, M, for each subject, which served as the RSFC matrix for each subject within each group.

### *Thresholding brain networks*

Thresholding an RSFC matrix is critical for obtaining a sparse adjacency matrix in that it should be optimal and

contain not too little functional connections for detecting group differences but not too many functional connections that it may dilute group differences. The most commonly used approach for thresholding is to globally threshold the RSFC matrix at a fixed threshold, $\rho$, for any $r_{ij}$ between $-1$ and 1. If $r_{ij} \geq \rho$, the corresponding element of the adjacency matrix, $M_{ij}$, is kept for the actual value of $r_{ij}$ for a weighted adjacency matrix or is set to be 1 for a binary adjacency matrix. If $r_{ij} < \rho$, then $M_{ij}$ is set to be 0 for both weighted and binary matrices. Note: except for strength, measures of modularity, local and global efficiency were computed using the binary adjacency matrix. One potential problem with this global thresholding method is that once thresholded, the sparse matrices are not fully connected from node to node (Alexander-Bloch et al., 2010). This disconnectedness of the resulting graphs may ultimately change the properties of the original global and local functional connectivity, which may bias the comparisons of graph-theoretic metrics between different groups of subjects.

In this study, we anticipated that this might be a factor affecting our observations in age-related differences in RSFC, and used a minimum spanning tree (MST) method in order to preserve fully connected brain graphs (Achard et al., 2012; Alexander-Bloch et al., 2010). In this study, each MST per subject is a spanning tree of a weighted subgraph that is fully connected with all nodes having a maximum total weight of all links. Although the MST sparsely represents a ''skeleton structure'' of the brain graph, it does not form clusters or loops at the regional level that keeps it from a biologically meaningful sparse representation (Alexander-Bloch et al., 2010). To obtain a sparse, fully connected, and biologically meaningful graph, we added extra links to the MST from the remaining adjacency matrix. To do so, for each final sparse adjacency matrix, we added top 2–40% of the remaining links to the MST, respectively, to include the highest proportion of the remaining functional connectivity. This ensured that each final graph per subject had an equal number of links, and, thus, observations on age-related group differences were independent of number of functional connections. Several values of the threshold were tested in order to examine the effect of different proportional thresholding on aging-related group differences. Thresholds from 2% to 40% were chosen based on the reasons that (1) the network measures are relatively constant over this range (Alexander-Bloch et al., 2010); (2) graphs become more random above a threshold level of 50% (Humphries et al., 2006). Current findings are based on thresholds from 2% to 8% at 2% intervals; results obtained from thresholds of 10% to 40% at 10% intervals can be found in the Supplementary Materials (Supplementary Figs. S1–S10; Supplementary Data are available online at www.liebertpub.com/brain).

### *Measures of graph metrics*

Graph metrics, including modularity, local and global efficiency, and strength, were estimated using the Brain Connectivity Toolbox (Rubinov and Sporns, 2010) with adaptation made for nodal or regional-level calculation. Previous studies have reported age-related changes in connectivity and network measures on a global or brain-wide level (Alexander-Bloch et al., 2010; Geerligs et al., 2014; Meunier et al., 2009a). In this study, network measures were estimated at global and regional level, thus enabling an examination of age-related changes in functional connectivity at a brain-wide level and at regional level for a finer-grained analysis. Global-level graph metrics were estimated by averaging each measure across all nodal regions and across all subjects in each group; regional level measures, except for modularity, were estimated for each node averaging across all subjects within each group. Statistical group comparison was conducted for each graph metric at each threshold using the Wilcoxon rank sum test.

Modularity is a global measure of how well a network can be decomposed into a set of sparsely interconnected but densely intraconnected modules (Newman, 2004) and can be a valuable tool in identifying the functional blocks within the brain network. The optimal modular structure for a given network is typically estimated with optimization algorithms rather than computed exactly (Danon et al., 2005; Rubinov and Sporns, 2010). In this study, network modularity was estimated via a two-step approach to achieve an optimal module division, similar to the one applied in other studies (Geerligs et al., 2014; Rubinov and Sporns, 2011). Modularity was first estimated using the Newman–Girvan algorithm (Newman, 2006a, 2006b). Each module is extracted as a group of nonoverlapping nodes by maximizing the number of within-module links and minimizing the number of between-module links among those nodes. Since the optimal community structure and maximized modularity may vary from run to run due to heuristics in the algorithm (Rubinov and Sporns, 2010), this step was repeated 500 times. In the second step, all previously detected community structures were refined using a fine-tuning algorithm (Rubinov and Sporns, 2010; Sun et al., 2009) with a maximum 500 times' iteration. Once an optimal modular structure of the network has been identified, it is possible to assign topological roles to each node based on its density of intra- and inter-modular connections (Guimera et al., 2005). Therefore, intramodular connectivity of each node was measured by the normalized intramodular degree, that is, the within-module degree $z$-score (Rubinov and Sporns, 2010). The within-module degree $z$-score is large for a node that has a large number of intramodular connections relative to other nodes in the same module. We used the measure of within-module degree $z$-score to identify those ''hub'' nodes with high intramodular connectivity and examined the age-related changes in these functionally important regions.

Local efficiency is a measure of information transfer in the immediate neighborhood of each node, indicating to what extent connections are being segregated into subnetworks (Achard et al., 2012), while global efficiency is a measure of information propagating in the whole network, indicating to what extent connections are being integrated into a whole brain-wide network (Rubinov and Sporns, 2010). These two measures are based on a pre-estimation of the minimum path length. For the local efficiency, the minimum path length is estimated as the shortest path length from node $i$ to its nearest neighbor node $j$ in the subgraph they both belong to. For the global efficiency, the minimum path length is estimated as the shortest path length from node $i$ to all other nodes $j$ in the whole graph.

The strength of functional connectivity of each node is measured as the mean value of weights (i.e., cross-correlation coefficients) of all functional connections linking to the

node. It provides an estimation of the functional importance of each node.

### *Measures of alteration of graph metrics*

Age-related topological changes are different across brain locations and networks. These patterns of changes cannot be truly reflected with a solely brain-wide examination. However, it might be visualized by plotting, for a given graph metric, the mean value at each node in the younger group versus the difference between the older and younger groups at each node. This approach was originally reported and used for detecting functional network changes in comatose patients, and the gradient of a straight line fitted to the data was referred to as a hub disruption index, $\kappa$ (Achard et al., 2012). In this study, the hub disruption index for a given graph metric, for example, strength, was constructed by subtracting the younger group mean nodal strength from the

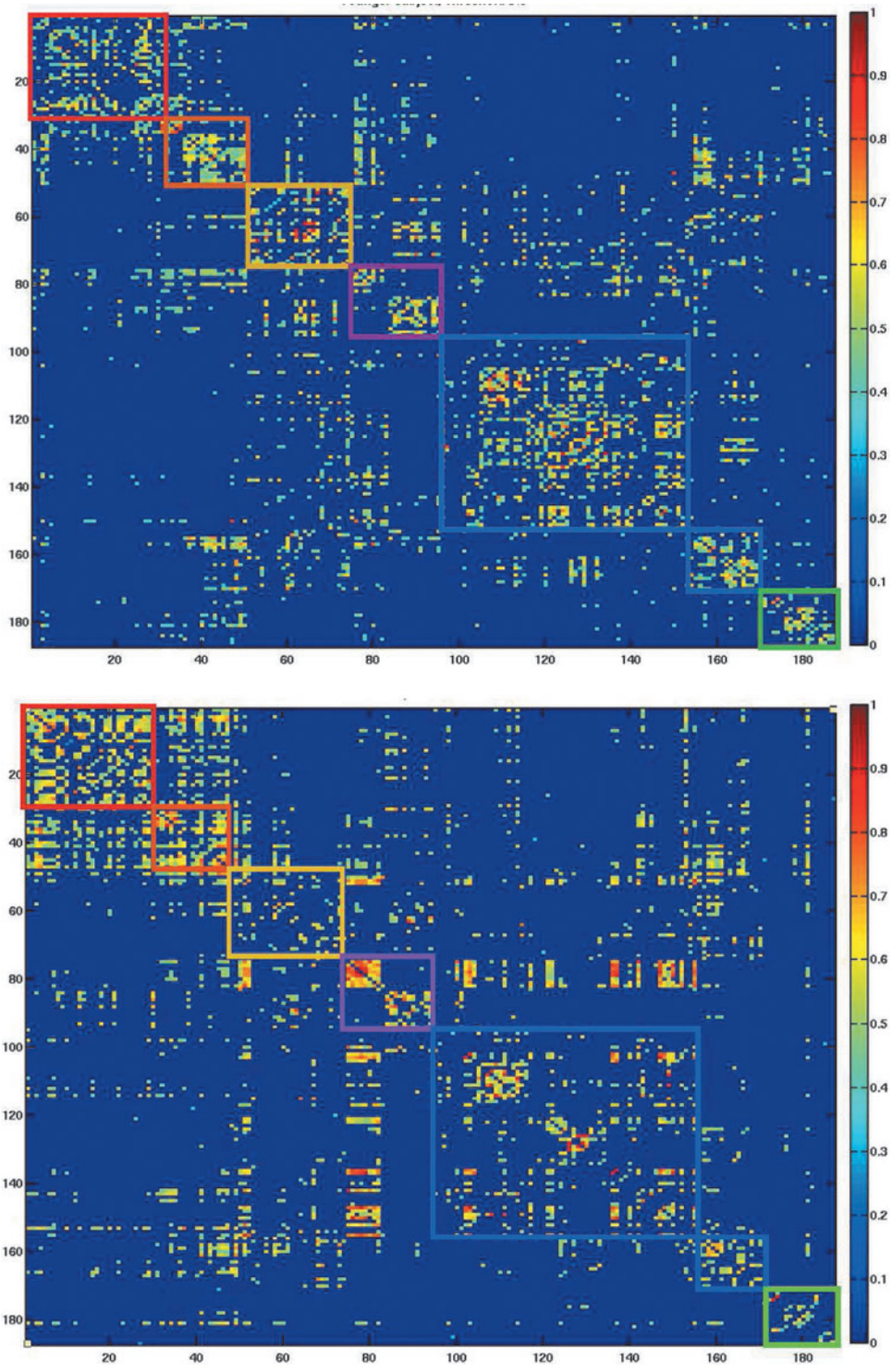


**FIG. 1.** Adjacency matrices shown at threshold of 8% (Young—upper panel, Older—bottom panel). Functional networks are illustrated using adjacency matrices. Rows and columns denote the 187 nodes, and each element of the matrix denotes a link between the corresponding nodes. Square blocks from the top left to the bottom right along the main diagonal represent the sensorimotor (red; 35 regions), cingulo-opercular task control (orange; 14 regions), fronto-parietal task control (gold; 25 regions), dorsal/ventral attention (magenta, 20 regions), default mode network (DMN; medium blue, 58 regions), salience network (royal blue; 18 regions), and subcortical/cerebellar (green; 17 regions) network. Elements within each block represent within-network functional connections and elements outside blocks represent between-network connections.

mean strength of the corresponding node in the older group and plotting this group mean difference against the younger group mean. This transformation improves visualization of the age-related differences in the profile of regional network properties.

## Results

### *Altered modularity with aging*

The functional networks representing patterns of cross-correlations between resting-state fMRI signals are illustrated using their adjacency matrices (Fig. 1). Rows and columns in these matrices denote the 187 nodes, while elements of each matrix denote links or the cross-correlations between the corresponding nodes. Major functional networks from the younger (top panel) and older (bottom panel) groups are represented along the main diagonal of adjacency matrices. From the top left to the bottom right along the main diagonal in Figure 1, the square blocks represent the functional network of the sensorimotor, cingulo-opercular task control, fronto-parietal task control, dorsal/ventral attention, DMN, salience network, and subcortical/cerebellar network.

At the global level, we observed that the mean modularity was reduced in the older group compared with the younger group over a range of different connection densities (Fig. 2a). The older group showed a higher variance of modularity across subjects compared with the younger group. Besides age-related differences in modularity between groups, both groups had mean values of modularity greater than 0.3 that were indicative of nonrandom community structure (Newman and Girvan, 2004). This further suggested the presence of modular structure of functional brain networks across the

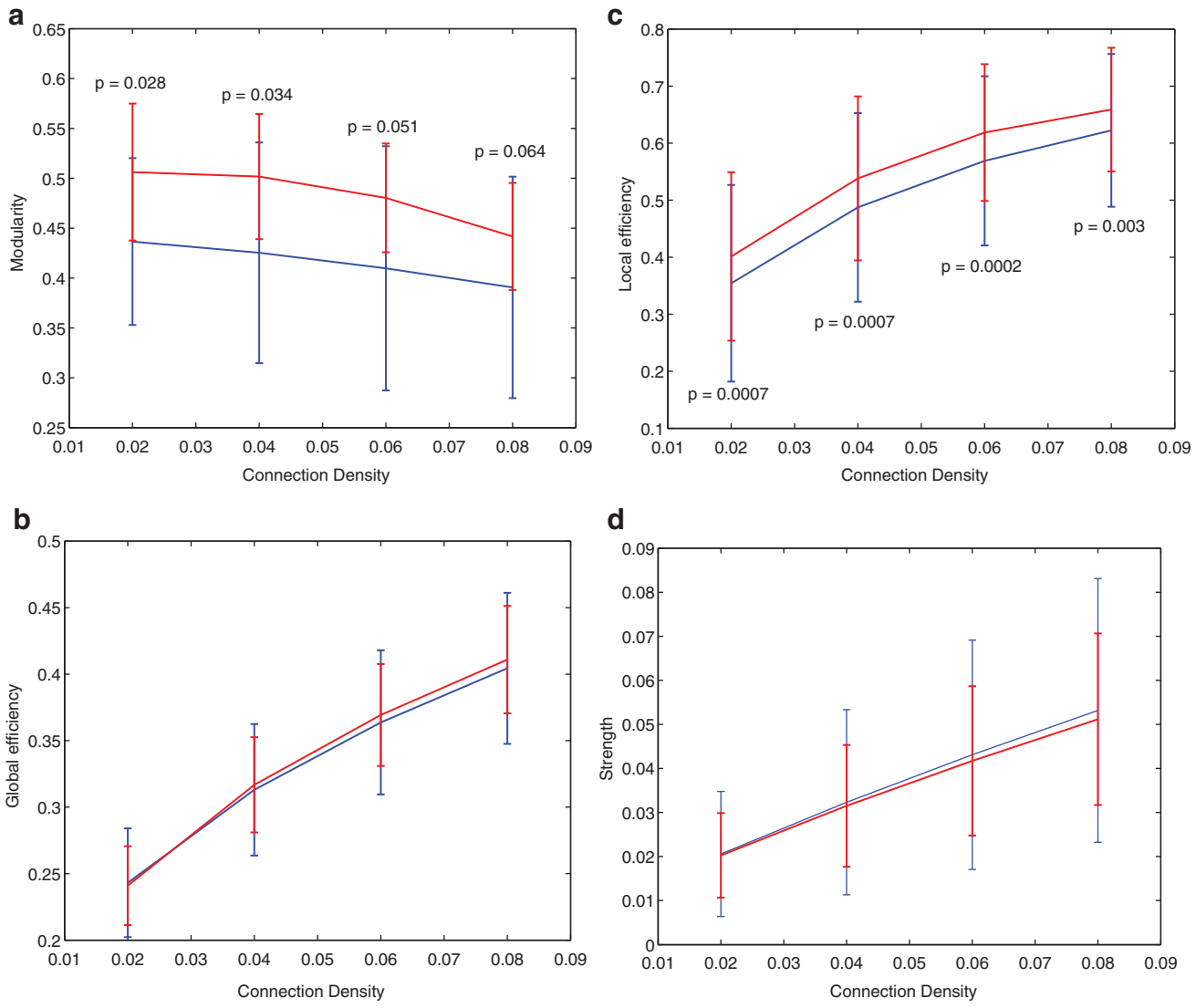


**FIG. 2.** **(a)** Modularity (Young—red; Older—blue). **(b)** Global efficiency (Young—red; Older—blue). **(c)** Local efficiency (Young—red; Older—blue). **(d)** Strength (Young—red; Older—blue). The older group (blue lines) showed decreased modularity and local efficiency compared with the young group (red lines) across a range of thresholds (i.e., connection density). Group comparison was tested using the Wilcoxon rank sum test with a *p*-value of significance shown at each threshold. No significant group difference was observed in the global efficiency and the strength of functional connectivity.

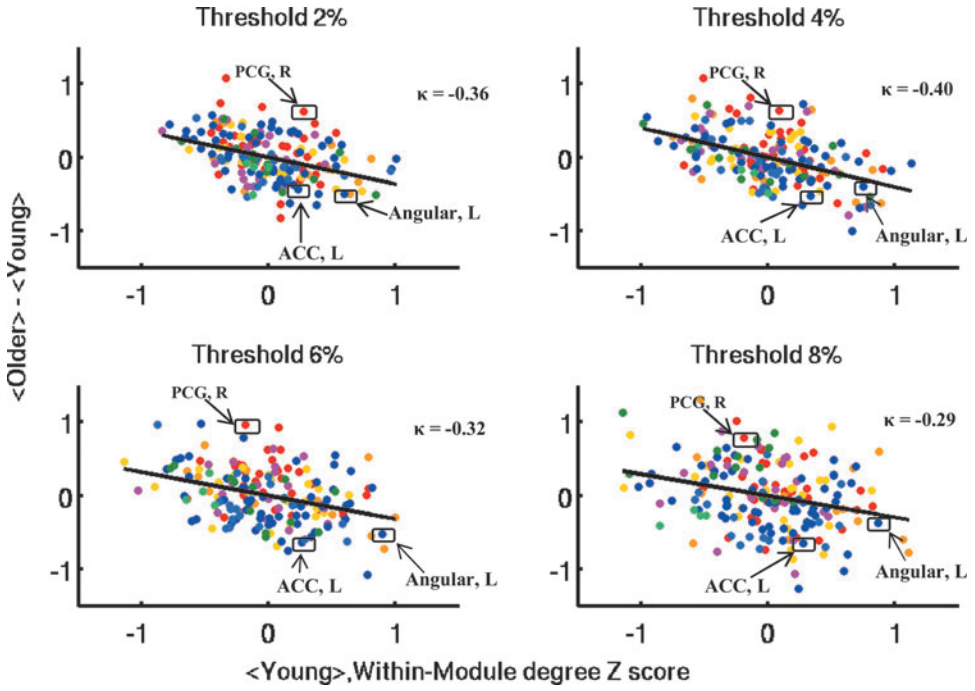


**FIG. 3.** Hub disruption index of within-module functional connectivity. The hub disruption index of within-module functional connectivity is plotted at each threshold of connection density. Each data point is color coded representing a node belonging to a particular functional network (i.e., red dots represent nodes belonging to the sensorimotor network, and blue dots represent nodes belonging to the DMN). The mean value of within-module degree *z*-score of each node in the younger group <Young> (*x*-axis) is plotted against the difference between groups in the mean value of within-module degree *z*-score of each node <Older> - <Young> (*y*-axis). A node with a high number of connections within a module (i.e., measured as within-module degree *z*-score) in the younger group showed an abnormal reduction of connections in the older group, for example, the left anterior cingulate cortex (ACC) and left angular gyrus (AG) from the DMN, whereas a node with a few within-module connections in the young group showed an abnormal increase of connections in the older group, for example, the right precentral gyrus (PCG) from the sensorimotor network. The solid black line represents a linear regression fitting to the data, and the slope of the line is defined as the hub disruption index, $\kappa$ (Achard et al., 2012). The negative hub disruption index across different levels of thresholding suggested an overall disruption of global modularity in the older group.

adult lifespan. For both groups, modularity declined monotonically as a function of increasing connection density (Fig. 2a).

At the nodal level, a negative hub disruption index was consistently observed for the measure of within-module degree *z*-score across different connection densities (Fig. 3). Nodes that had dense intramodular connections in the younger group (i.e., left anterior cingulate cortex [ACC] and left angular gyrus [AG]) were sparsely connected to other nodes within the same module in the older group, whereas nodes which had fewer intramodular connections in the younger group (i.e., right precentral gyrus [PCG]) were densely connected to other nodes within the same module in the older group.

### *Altered efficiency of functional connectivity with aging*

At the whole-brain level, global efficiency was not significantly different between the two groups (Fig. 2b) with hub disruption indices close to zero (Fig. 4), while local efficiency was significantly reduced in the older group over a range of different connection densities (Fig. 2c). The older group also showed a higher variance of local efficiency compared with the younger group. Besides age-related differences in efficiency measures between the two groups, we observed that efficiency increased monotonically as a function of increasing connection density (Fig. 2b, c) for both groups.

At the nodal level, we observed markedly different patterns of age-related changes in network efficiency depending on the functional properties of individual brain regions. Both global and local efficiency was decreased in the DMN but increased in the sensorimotor network (Figs. 4 and 5 and Supplementary Figs. S11 and S12). Our results also showed a negative hub disruption index for the measure of local efficiency (Fig. 5), suggesting a potential age-induced exchange of a hub region with a nonhub region or vice versa.

### *Altered functional connectivity strength with aging*

At the global level, the older group showed higher functional connectivity strength but not significantly different from the younger groups (Figs. 2d and 6). At the global level, the hub disruption index of strength was 0.03, 0.11, 0.16, and 0.19 for thresholds of connection density at 2%, 4%, 6%, and 8%, respectively (Fig. 7). Small positive values of the hub disruption indices correspond to the slightly higher functional connectivity strength observed in Figures

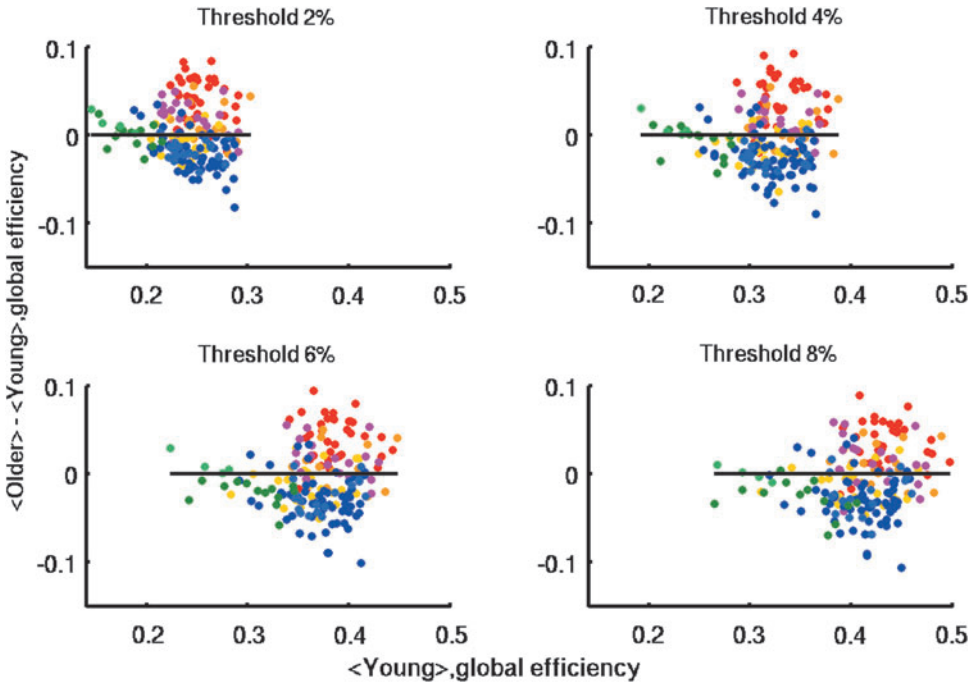


**FIG. 4.** Hub disruption index of global efficiency. In the figure, each black horizontal line represents equivalent global efficiency for the older group versus the younger group. The hub disruption index of global efficiency was close to zero. However, nodes belonging to the sensorimotor network (red) showed increased global efficiency consistently, while nodes belonging to the DMN (medium blue) showed decreased global efficiency consistently.

2d and 6. At the regional level, we observed prominent group differences in the DMN and the sensorimotor network (Fig. 7). Within the DMN, we found decreased within-network strength (Fig. 8a) and a negative hub disruption index (Fig. 9) with aging. In contrast, we found increased strength within the sensorimotor network (Figs. 8b and 10a) and an overall increase in functional connectivity strength between the sensorimotor network and all other networks (Fig. 10b), particularly between the sensorimotor and attention networks (Fig. 10c).

*Age-related reorganizational changes in functional brain networks*

Brain reorganization with aging undergoes dynamic changes across different functional brain networks. We further conducted a secondary analysis to quantify the changes in each brain network using strength and degree (Supplementary Figs. S13 and S14). Degree is a binary measure of functional connectivity and is estimated as the number of functional connections that survived thresholding. These two measures provide

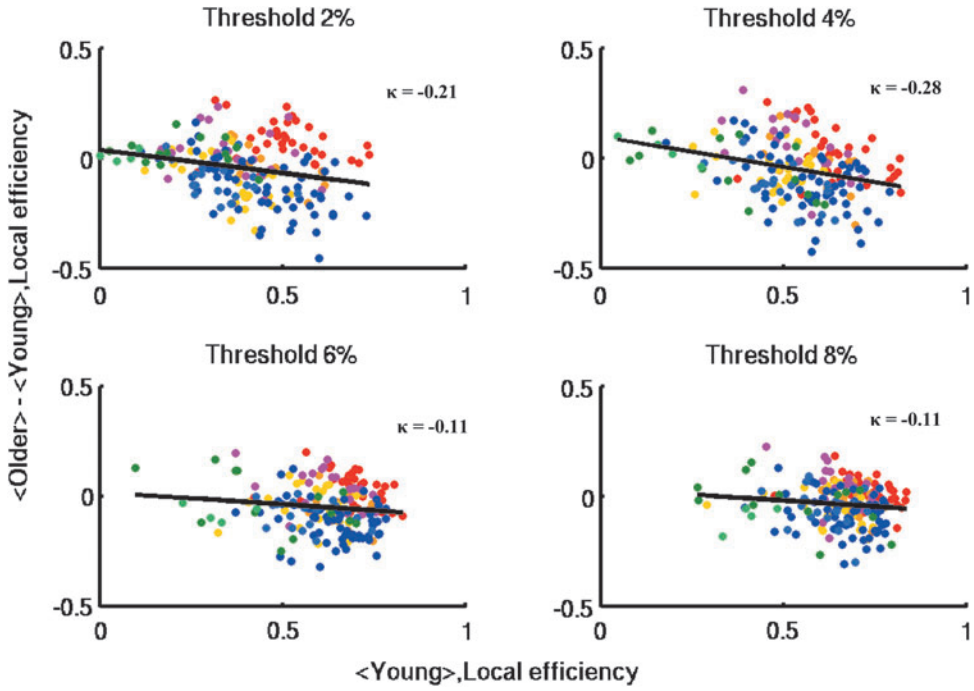


**FIG. 5.** Hub disruption index of local efficiency. The hub disruption index of local efficiency is plotted at each threshold of connection density. The mean value of local efficiency of each node in the younger group <Young> (*x*-axis) is plotted against the difference between groups in mean local efficiency of each node <Older> - <Young> (*y*-axis). The hub disruption index of local efficiency was estimated as the gradient of the solid black line fitted to the scatterplots. Negative hub disruption indices were observed across different thresholds, indicating an overall disruption of local efficiency in the older group. The sensorimotor network (red dots) and the DMN (blue dots) are the two most distinguishable networks showing consistent disruption.

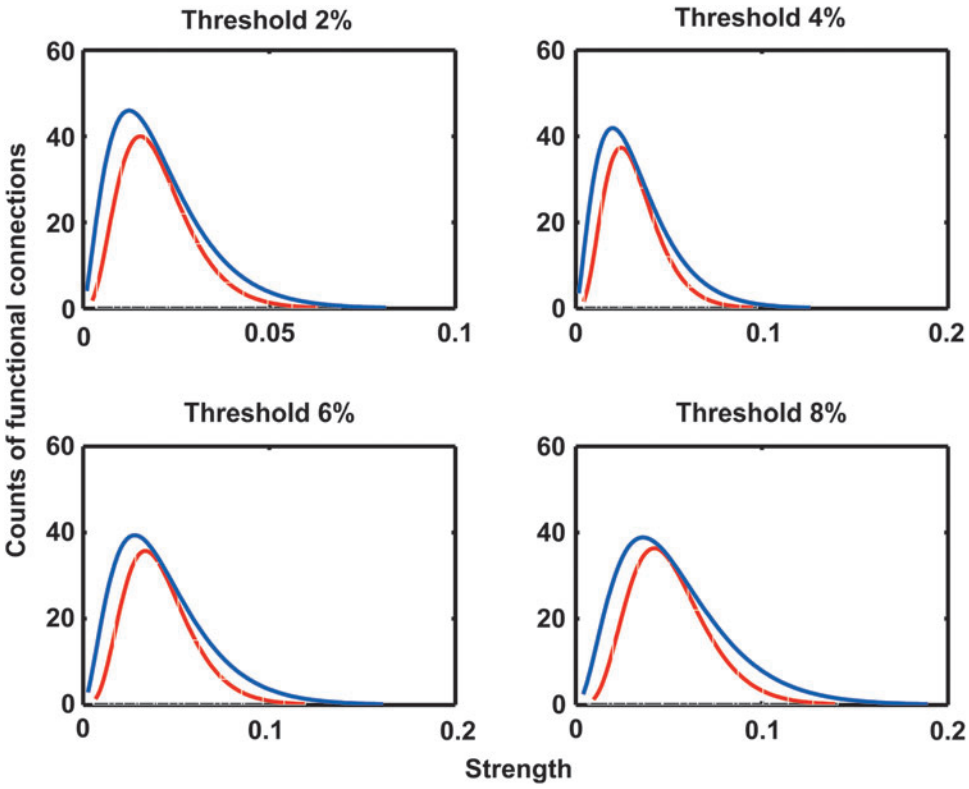


**FIG. 6.** Distribution of functional connectivity strength (Young—red; Older—blue). The figure illustrates the distribution of functional connectivity strength compared between the two groups (histogram with a gamma distribution fit; older group—blue lines; young group—red lines).

complementary aspects of network organization. Proportional tests were used to compare the proportions of strength and degree of each network to the total strength and degree in whole-brain networks, respectively. FDR correction was applied for multiple comparisons (Benjamini and Hochberg, 1995).

We again observed distinct patterns of age-related reorganization in the DMN and the sensorimotor network (Supplementary Figs. S13 and S14 and Table 1). Within the DMN (i.e., elements within the square block of the RSFC matrices representing the DMN), both the strength (adjusted $p$-value = 0.024; Supplementary Fig. S13a) and degree (adjusted $p$-value = 0.0005; Supplementary Fig. S14a) significantly decreased with aging. In contrast, within the sensorimotor network, both the strength (adjusted $p$-value = 0.024; Supplementary

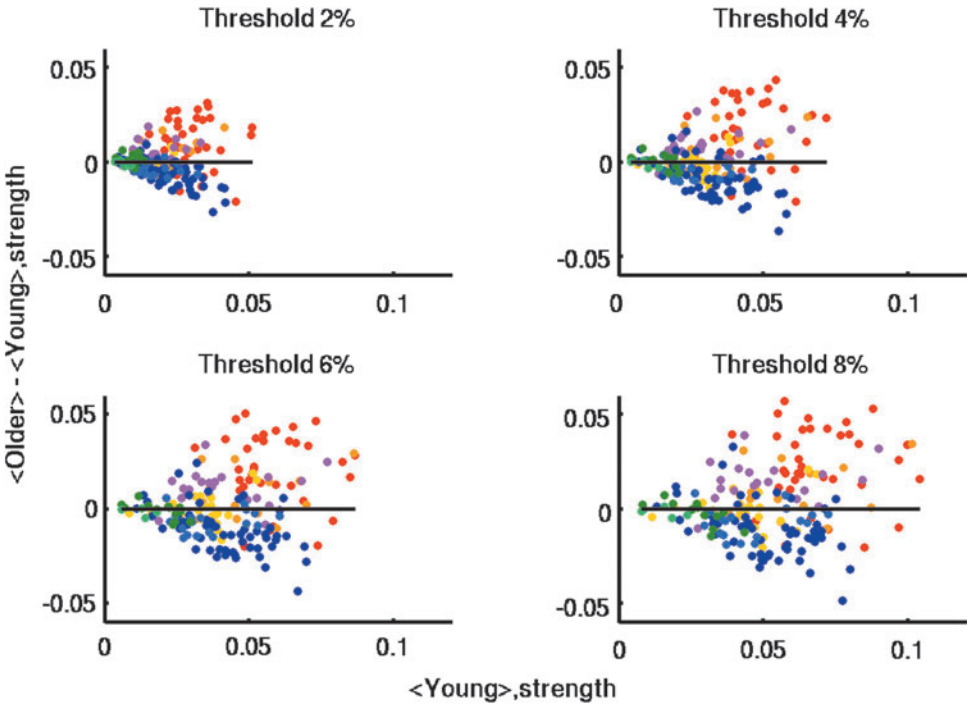


**FIG. 7.** Hub disruption index of strength. In the figure, each black horizontal line represents equivalent function connectivity strength estimated for the older group versus the younger group. However, nodes belonging to the sensorimotor network (red) showed increased strength consistently, while nodes belonging to the DMN (medium blue) showed decreased strength.

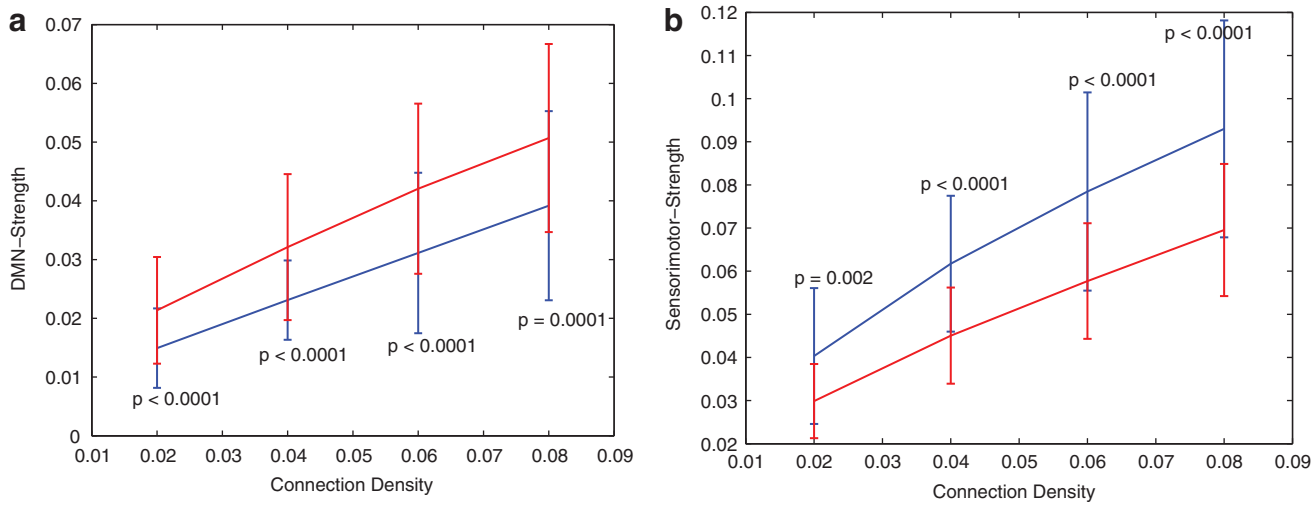


**FIG. 8.** Age-related changes in functional connectivity strength. **(a)** Within the DMN (Young—red; Older—blue). **(b)** Within the sensorimotor network (Young—red; Older—blue). Differences of functional connectivity strength within the DMN **(a)** and the sensorimotor network **(b)** between the older (blue lines) and younger group (red lines) are plotted across different thresholds of connection density. Significantly decreased strength within the DMN ($p$-value $\leq 0.0001$) and increased strength within the sensorimotor network ($p$-value $< 0.01$) was observed in the older group (Wilcoxon rank sum test).

Fig. S13a) and degree (adjusted $p$-value $= 0.005$; Supplementary Fig. S14a) significantly increased with aging. Between networks (i.e., the off-diagonal elements of the RSFC matrices), no significant age-related changes were observed in functional strength of between-network connections. However, the number of functional connections between the sensorimotor and all other networks significantly increased with aging (adjusted $p$-value $< 0.00001$; Supplementary Fig. S14b, c). We also observed significantly increased between-network connections in the subcortical network (adjusted $p$-value $= 0.005$) in the older group (Supplementary Fig. S14b, c). The older group showed a significantly decreased proportion of between-network connections in both the frontal-parietal and salience networks (adjusted $p$-value $< 0.01$; Supplementary Fig. S14b, c).

## Discussion

In this study, we used the correlations derived from the resting-state fMRI BOLD signals to develop a network model of the brain in two representative groups of healthy individuals. Graph-theory based network analysis was applied to examine age-related brain network reorganization. We found that similar to other studies (Bassett et al., 2010; Geerligs et al., 2014; Meunier et al., 2009a; 2009b), the functional

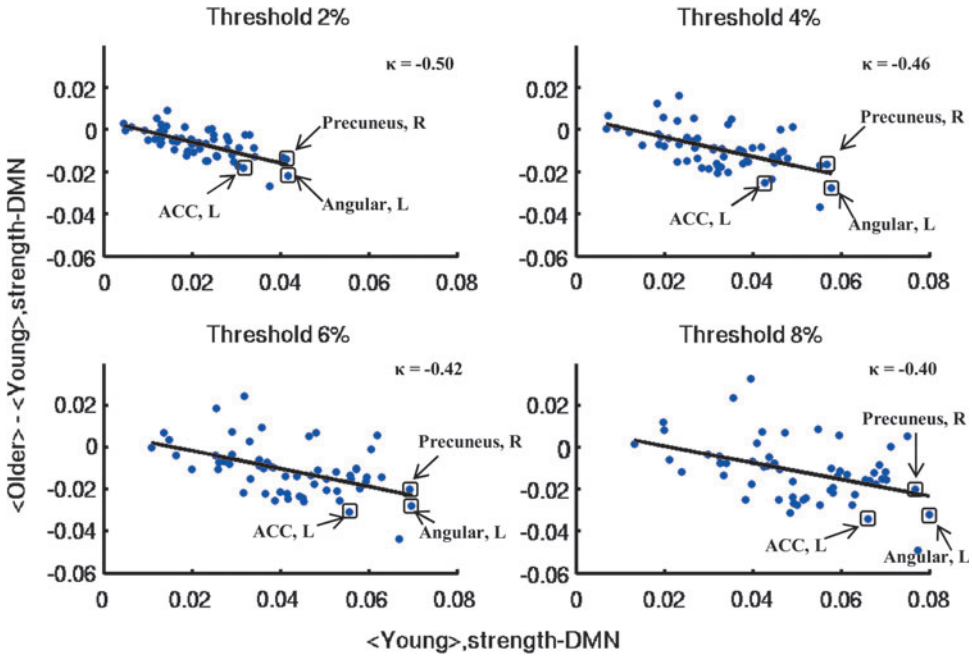


**FIG. 9.** Hub disruption index of strength–DMN. For all nodes belonging to the DMN, the mean value of strength of each of these nodes in the younger group $<$Young$>$ ($x$-axis) is plotted against the difference between groups in mean strength of each node $<$Older$>$ - $<$Young$>$ ($y$-axis). The hub disruption index of strength was estimated as the gradient of the solid black line fitted to the scatterplots. The left angular gyrus (AG), left ACC, and the right precuneus strongly connected to all other nodes within the DMN in the younger group, and showed reduced regional strength in the older group.

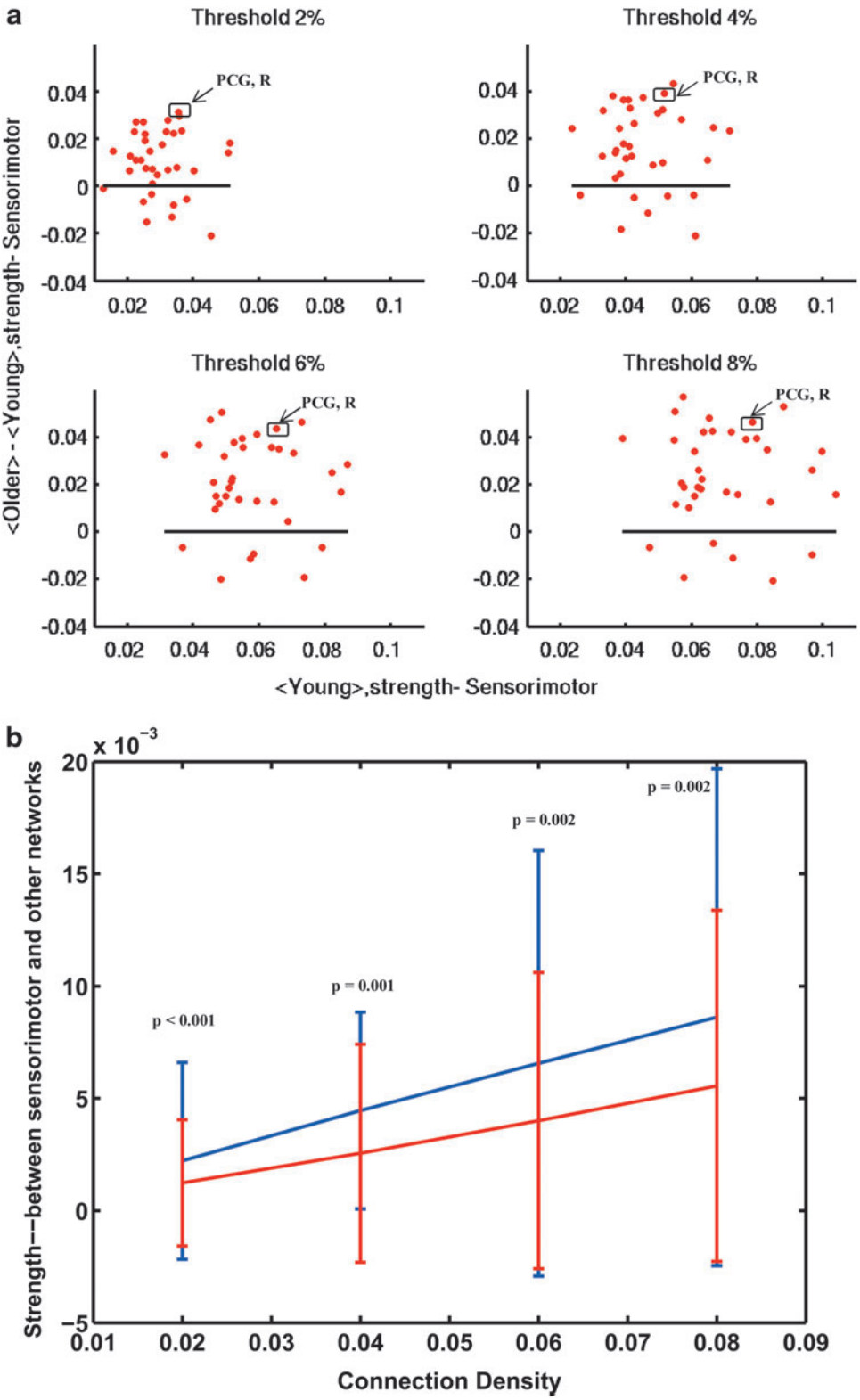


**FIG. 10.** Changes in functional strength in the sensorimotor network**. (a)** Within the sensorimotor network. The red horizontal line represents equivalent strength within the sensorimotor network estimated for the older group versus the younger group. The majority of sensorimotor regions showed increased strength in the older group (i.e., above the horizontal zero line) such as the PCG, showing strengthened connections in the older group. **(b)** Between the sensorimotor network and all other networks. Group differences of functional connectivity strength between the sensorimotor network and all other networks are plotted across different thresholds of connection density (older group-blue line, younger group-red line). Significantly increased strength between the sensorimotor and all other networks ($p$-value $< 0.01$) was observed in the older group (Wilcoxon rank sum test). **(c)** Hub disruption between the sensorimotor network and all other networks. The figure shows age-related regional changes in functional connectivity strength between the sensorimotor and all other networks. Positive hub disruption indices are indicated by the slope of the solid black line fitted to each scatter plot. The dorsal/ventral attention network (magenta) showed strengthened connections to the sensorimotor network.

brain networks of both groups exhibited modular organization (Fig. 1). Graph theoretical work has shown that the human brain consists of modular structures (Bassett et al., 2010; Meunier et al., 2009b) which are altered in different clinical conditions such as Schizophrenia (Alexander-Bloch et al., 2010), Alzheimer's disease (AD) (Brier et al., 2014), and in normal aging (Geerligs et al., 2014; Meunier et al., 2009a). This study was partly motivated by a recent work exploring brain network topology in comatose patients (Achard et al., 2012) based on graph metrics estimated from each individual brain region in the network. We adopted a similar approach to conduct a finer-grained analysis of

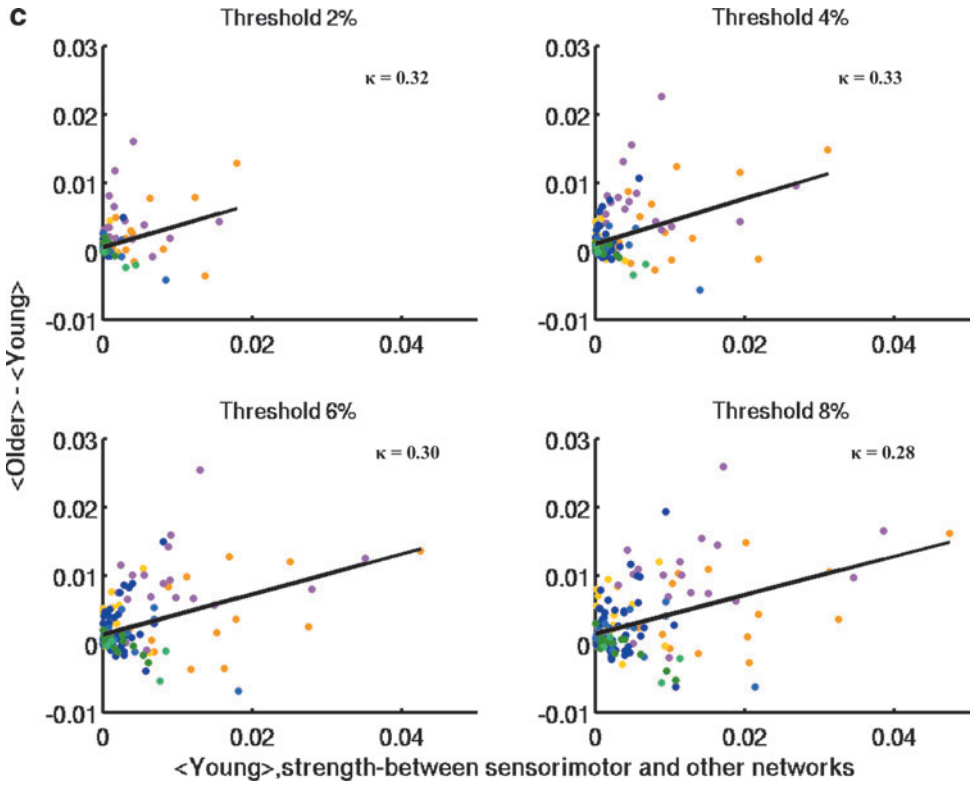


**FIG. 10.** (Continued).

changes in brain functional reorganization associated with aging along with a systematic brain-wide network analysis. These findings are summarized in Table 2.

### *Thresholding effect on brain network analysis*

Several levels of threshold were tested in order to examine the effect of different proportional network thresholding on aging-related group differences. One way to control the thresholding effect is by evaluating the modularity measure. We observed both groups showing minimal values of modularity greater than 0.3 by the threshold level of 8% with total 187 brain regions, which were indicative of nonrandom community structure (Newman and Girvan, 2004). In addition, modularity and local efficiency were significantly different between the two groups at a threshold level of 2% to 4%. Therefore, in this study, with 187 brain regions and the MST method, a threshold level of top 2% to 4% of connections with the highest functional strength provided a clear picture of network differences between the young and old groups.

### *Modularity decreases with healthy aging*

The modular organization of human brain has been discussed in previous and recent studies (Eccles, 1981; Gomez-Robles et al., 2014; Szentagothai, 1975). Several studies have reported that the modular organization could be affected under neuropsychological conditions and disorders, including depression (Peng et al., 2014), Schizophrenia (Alexander-Bloch et al., 2014), epilepsy (Xu et al., 2013), and age-related neurodegenerative diseases such as Parkinson's disease (Gottlich et al., 2013) and AD (Kikuchi et al., 2013). One study also observed age-related alterations in the modular organization using cortical thickness analysis (Chen et al., 2011). Therefore, in our study, we hypothesized that the brain functional modular structure can be affected by aging. We further observed a reduced modularity in the older group (Fig. 2a). This age-related decline in modularity indicates a less differentiated functional modular structure associated with aging. This alteration could be due to two main factors—an increase in intermodular connections or a decrease in intramodular connections or a mix of the two factors. To further test this, we used the measure of hub

Table 1. Age-Related Network Reorganization in the Sensorimotor and Default Mode Network

| *Network measures* | *Within-network* | | *Between-network* | |
|---|---|---|---|---|
| | *DMN* | *Sensorimotor* | *DMN* | *Sensorimotor* |
| Strength | ↓ | ↑ | → | → |
| Degree | ↓ | ↑ | → | ↑ |

Arrows indicate directional changes of network measures with aging.
DMN, default mode network.

Table 2. Age-Related Network Reorganization

| *Network measures* | *Effect of aging* |
|---|---|
| Modularity | ↓ |
| Local efficiency | ↓ |
| Global efficiency | → |
| Strength | → |

Arrows indicate directional changes of network measures with aging.

Table 3. Group Comparisons of Strength and Degree from Whole-Brain Network Analysis

| | *Strength* | | | *Degree* | | |
|---|---|---|---|---|---|---|
| | *Within network* | *Between network* | *Total* | *Within network* | *Between network* | *Total* |
| Young | 234.34 | 118.07 | 352.41 | 1822 | 1781 | 3603 |
| Older | 211.58↓ | 146.32↑ | 357.90↑ | 1642↓ | 2186↑ | 3828↑ |

Arrows indicate directional changes of network measures with aging.

disruption index to quantify the within-module functional connectivity at the regional level. We found a consistent regional alteration of modularity in the older group over a range of different thresholds (Fig. 3). Brain regions, such as left ACC and left AG as a part of the DMN, which had dense within-module connections in the younger brain networks, had fewer within-module connections in the older group, whereas regions, such as right PCG, a part of the sensorimotor network, which were sparsely connected to other regions within a module in the younger group, were densely connected in the older group. This regional alteration can be explained as the exchange of high-degree hub regions to low-degree nonhub regions or vice versa due to the effect of aging. This alteration of the order of importance of specific cortical regions within the same module indicates that although the whole-brain network could be equally well decomposed into a set of modules in both groups, especially at higher thresholds (i.e., modularity was not significantly different between the two groups at threshold $>6\%$), functional identity of individual brain regions comprising specific modules might have markedly changed due to the effect of aging.

Interestingly, although we observed an overall reduction of within-module functional connections in the older group, the total strength of functional connectivity seems increased in the older group (Fig. 6), although not reaching statistical significance. To further explore this, we constructed a group-level whole-brain network by averaging each individual network across all subjects within each group and then calculated the strength and the number of within-network connections and between-network connections. Results presented here are based on a threshold level of top 2%. We found that the older group had fewer within-network connections but more between-network connections compared with the younger group (Table 3). This suggests that whole-brain level increased functional connectivity between networks, which might be related to the over-activations in the elderly caused by less efficient use of neural resources (Geerligs et al., 2014; Morcom et al., 2007; Rypma et al., 2007). A detailed group comparison of strength and degree for each individual network can be found in the Supplementary Figures S13 and S14.

### *Reduced local efficiency but stable global efficiency with aging*

Local efficiency was decreased in the older group (Fig. 2c), while global efficiency was not affected by aging (Fig. 2b). Local efficiency is a measure of local information processing. As discussed earlier, the whole brain-wide reduction of within-module connections in the elderly might lead to an over-recruitment of brain regions in order to process the seemingly overwhelming incoming information, which leads to less efficiency (Morcom et al., 2007; Rypma et al., 2007). However, global efficiency is statistically stable between the two groups. This might be due to the equivalent amount of shortest path length for long-distance information processing in both groups (aided by the counterbalance of less within-network connections but more between-network connections in the older group). This observation has some bearing on the neural bases for the pervasive age-related slowing effects on cognitive performance based on the processing-speed theory (Salthouse, 1996). This theory suggests that cognitive performance is degraded when processing is slow, because relevant operations cannot be successfully executed in limited time. This might be reflected by age-related reduction in local efficiency, which constrains the efficiency or effectiveness of specific processes of local information transfer. However, some relevant limitations may be partially overcome by experience, as one view of expertise is that it serves to circumvent processing constraints or limitations (Salthouse, 1991), which may be associated with the stable measurement of global efficiency observed in both age groups. At the regional level, local efficiency tends to decrease with a negative hub disruption index (Fig. 5), which is consistent with the brain-wide decreased local efficiency. Global efficiency examined at the regional level does not show significant group differences (Fig. 4). However, both regional measures demonstrate distinct patterns of alteration in two important functional networks—the DMN and the sensorimotor network, which highlights the importance of examining brain reorganization at the regional level as brain regions making up the different functional modules undergo different changes that may not be observed at the brain-wide level. Measures of local efficiency and global efficiency are decreased in the DMN but increased in the sensorimotor network (Figs. 4 and 5 and Supplementary Figs. S11 and S12).

The DMN is a nonhuman-specific intrinsic functional network, active all over the life from birth until aging where it is progressively modified, sensitive to different pathologies, including AD, multiple sclerosis, and mild cognitive impairment (MCI), and is known for its role in supporting high-level cognitive functions (Gili et al., 2011; Mevel et al., 2010). The reduced efficiency in both local and global information processing in the DMN in relation to aging directly reflects a decreased functional connectivity as observed in previous studies (Damoiseaux et al., 2008; Hafkemeijer et al., 2012) and in our study (Fig. 8a). The decrease in functional connectivity leading to a decreased local and global efficiency may lead to the commonly observed age-related cognitive decline in patients with MCI and in the early stages of AD, two clinical conditions in which DMN shows

decreased functional connectivity (Greicius et al., 2004; Sorg et al., 2007). The sensorimotor network, associated with primary information processing, showed increased local and global efficiency. This finding is consistent with the hypothesis that cognitive systems should compensate in aging for the general decline in sensorimotor abilities (Li and Lindenberger, 2002; Seidler et al., 2010) as well as decreased functional connectivity and efficiency in DMN.

### *Altered functional connectivity in the DMN and the sensorimotor network*

The measure of strength of functional connectivity is highly consistent with all observations we have discussed. This is not surprising, as we also found that the regional strength of functional connectivity was significantly decreased in the DMN and increased in the sensorimotor network (Table 1 and Figs. 7 and 8). With the same number of functional connections, although brain-wide strength of RSFC seems to be higher in the older group (Fig. 6), it is not significantly different between groups (Fig. 2d). At the regional level, the strength of functional connectivity showed a similar pattern of changes in the DMN and sensorimotor networks as observed in the measures of local and global efficiency (Fig. 7). The negative hub disruption index observed in the DMN indicates an exchange of hub to nonhub regions (Fig. 9). This regional reorganization reveals a shift of functional importance of individual regions with aging and within the same functional module, which may not be easily observed in a brain-wide network analysis. We observed that left ACC, left AG, and right precuneus as a part of the DMN switched from a hub region to a nonhub region with aging. These regions are associated with cognitive function (Pardo et al., 2007; Seghier, 2013) and have shown decreased functional connectivity in AD patients (Hafkemeijer et al., 2012).

One previous study used the test-retest reliability approach to examine age-related differences in RSFC and demonstrated increased reliable functional connections within the sensorimotor network in the older group (Song et al., 2012). Here, we observed an overall increase in functional connectivity across all regions belonging to the sensorimotor network (Fig. 10a). Given that another previous study also observed an increase in functional connectivity between the sensorimotor and task-control networks (Meier et al., 2012), we further examined the connections between sensorimotor and all other networks in this study. We found a positive hub disruption index, indicating increased connections between the sensorimotor network and other networks in the older group, particularly between the sensorimotor and attention networks. This was further confirmed by the observation of an increased number of connections and strength between these two networks (Supplementary Table S1). This finding suggests that the attention network and the sensorimotor network have become less differentiated in normal aging, contributing to the reduced modularity, possibly due to the greater functional interdependence of these networks in the elderly.

This study has limitations. The number of subjects is not large, with 16 subjects in each group. It is possible that the lack of significance for group comparison in brain-wide network analysis may be due to inadequate statistical power. However, we were able to uncover group differences at the regional level. As we mentioned earlier, the adult brain has shown shrinkage as it ages. The structural changes may have an impact on the results of functional connectivity and network analysis. For future studies, an examination of the regional network measures combined with local gray matter volume and the subject's performance in cognitive tests may provide a better understanding of age-related brain functional reorganization.

## Conclusion

In this study we have shown that the human brain undergoes functional reorganization with aging at a whole brain-wide level and a regional level. The brain-wide network analysis showed reduced modularity and local efficiency in the older group, possibly related to decreased within-network connections. We also conducted regional-level network analysis for a finer-grained examination of age-related brain reorganization. We have shown that individual brain regions underwent distinct patterns of reorganization in terms of their functional properties. Brain regions in the DMN showed reduced local and global efficiency as well as regional functional connectivity, indicating a decline in high-level cognitive functioning with aging, while an increase in these measures was observed in the sensorimotor network in the older group, possibly indicating an underlying compensation mechanism for declined sensorimotor and cognitive abilities. Regional alteration also revealed a switch of functional importance of individual brain regions from a hub region to a nonhub region or vice versa. Our results suggest that brain-wide topological properties, such as modularity, are able to provide insights of brain network reorganization, but with a finer-grained analysis at the regional level; more specific details of how individual brain regions with different functional properties evolve with aging are able to provide a better understanding of the aging brain.

## Acknowledgments

The authors thank all subjects for their participation. Portions of this work were previously presented in poster form at the 20th Annual Meeting of the Organization for Human Brain Mapping Annual Meeting. This work was supported by NIH grants RC1MH090912-01, K23NS086852, T32GM008692, UL1TR000427, and T32EB011434, by a Coulter Translational Research Award, an American Heart Association Postdoctoral Fellow Research Award, UW Milwaukee-Madison Intercampus Grants, and by Grants from the Shapiro Foundation and Foundation of ASNR award.

## Author Disclosure Statement

No competing financial interests exist.

## References

Achard S, Delon-Martin C, Vertes PE, Renard F, Schenck M, Schneider F, Heinrich C, Kremer S, Bullmore ET. 2012. Hubs of brain functional networks are radically reorganized in comatose patients. Proc Natl Acad Sci U S A 109: 20608–20613.

Alexander-Bloch AF, Gogtay N, Meunier D, Birn R, Clasen L, Lalonde F, Lenroot R, Giedd J, Bullmore ET. 2010. Disrupted modularity and local connectivity of brain functional

networks in childhood-onset schizophrenia. Front Syst Neurosci 4:147.
Alexander-Bloch AF, Reiss PT, Rapoport J, McAdams H, Giedd JN, Bullmore ET, Gogtay N. 2014. Abnormal cortical growth in schizophrenia targets normative modules of synchronized development. Biol Psychiatry 76:438–446.
Bassett DS, Greenfield DL, Meyer-Lindenberg A, Weinberger DR, Moore SW, Bullmore ET. 2010. Efficient physical embedding of topologically complex information processing networks in brains and computer circuits. PLoS Comput Biol 6:e1000748.
Benjamini Y, Hochberg Y. 1995. Controlling the false discovery rate— a practical and powerful approach to multiple testing. J R Stat Soc Ser B Methodol 57:289–300.
Birn RM, Molloy EK, Patriat R, Parker T, Meier TB, Kirk GR, Nair VA, Meyerand ME, Prabhakaran V. 2013. The effect of scan length on the reliability of resting-state fMRI connectivity estimates. Neuroimage 83:550–558.
Brier MR, Thomas JB, Fagan AM, Hassenstab J, Holtzman DM, Benzinger TL, Morris JC, Ances BM. 2014. Functional connectivity and graph theory in preclinical Alzheimer's disease. Neurobiol Aging 35:757–768.
Chen ZJ, He Y, Rosa-Neto P, Gong GL, Evans AC. 2011. Age-related alterations in the modular organization of structural cortical network by using cortical thickness from MRI. Neuroimage 56:235–245.
Cox RW. 1996. AFNI: software for analysis and visualization of functional magnetic resonance neuroimages. Comput Biomed Res 29:162–173.
Damoiseaux JS, Beckmann CF, Arigita EJ, Barkhof F, Scheltens P, Stam CJ, Smith SM, Rombouts SA. 2008. Reduced resting-state brain activity in the default network in normal aging. Cereb Cortex 8:1856–1864.
Danon L, Diaz-Guilera A, Duch J, Arenas A. 2005. Comparing community structure identification. J Stat Mech Theory Exp 2005:P09008. DOI: 10.1088/1742-5468/2005/09/P09008.
Eccles JC. 1981. The modular operation of the cerebral neocortex considered as the material basis of mental events. Neuroscience 6:1839–1855.
Geerligs L, Renken RJ, Saliasi E, Maurits NM, Lorist MM. 2014. A brain-wide study of age-related changes in functional connectivity. Cereb Cortex [Epub ahead of print]; DOI: 10.1093/cercor/bhu012.
Gili T, Cercignani M, Serra L, Perri R, Giove F, Maraviglia B, Caltagirone C, Bozzali M. 2011. Regional brain atrophy and functional disconnection across Alzheimer's disease evolution. J Neurol Neurosurg Psychiatry 82:58–66.
Gomez-Robles A, Hopkins WD, Sherwood CC. 2014. Modular structure facilitates mosaic evolution of the brain in chimpanzees and humans. Nat Commun 5:4469.
Gottlich M, Munte TF, Heldmann M, Kasten M, Hagenah J, Kramer UM. 2013. Altered resting state brain networks in Parkinson's disease. PLoS One 8:e77336.
Greicius MD, Srivastava G, Reiss AL, Menon V. 2004. Default-mode network activity distinguishes Alzheimer's disease from healthy aging: evidence from functional MRI. Proc Natl Acad Sci U S A 101:4637–4642.
Guimera R, Mossa S, Turtschi A, Amaral LAN. 2005. The worldwide air transportation network: anomalous centrality, community structure, and cities' global roles. Proc Natl Acad Sci U S A 102:7794–7799.
Hafkemeijer A, van der Grond J, Rombouts SA. 2012. Imaging the default mode network in aging and dementia. Biochim Biophys Acta 1822:431–441.
Hagmann P, Cammoun L, Gigandet X, Meuli R, Honey CJ, Wedeen VJ, Sporns O. 2008. Mapping the structural core of human cerebral cortex. PLoS Biol 6:e159.
Humphries MD, Gurney K, Prescott TJ. 2006. The brainstem reticular formation is a small-world, not scale-free, network. Proc Biol Sci 273:503–511.
Jones TB, Bandettini PA, Kenworthy L, Case LK, Milleville SC, Martin A, Birn RM. 2010. Sources of group differences in functional connectivity: An investigation applied to autism spectrum disorder. Neuroimage 49:401–414.
Kikuchi M, Ogishima S, Miyamoto T, Miyashita A, Kuwano R, Nakaya J, Tanaka H. 2013. Identification of unstable network modules reveals disease modules associated with the progression of Alzheimer's disease. PLoS One 8:e76162.
Li KZ, Lindenberger U. 2002. Relations between aging sensory/sensorimotor and cognitive functions. Neurosci Biobehav Rev 26:777–783.
Meier TB, Desphande AS, Vergun S, Nair VA, Song J, Biswal BB, Meyerand ME, Birn RM, Prabhakaran V. 2012. Support vector machine classification and characterization of age-related reorganization of functional brain networks. Neuroimage 60:601–613.
Meunier D, Achard S, Morcom A, Bullmore E. 2009a. Age-related changes in modular organization of human brain functional networks. Neuroimage 44:715–723.
Meunier D, Lambiotte R, Fornito A, Ersche KD, Bullmore ET. 2009b. Hierarchical modularity in human brain functional networks. Front Neuroinform 3:37.
Mevel K, Grassiot B, Chetelat G, Defer G, Desgranges B, Eustache F. 2010. The default mode network: cognitive role and pathological disturbances. Rev Neurol (Paris) 166:859–872.
Morcom AM, Li J, Rugg MD. 2007. Age effects on the neural correlates of episodic retrieval: increased cortical recruitment with matched performance. Cereb Cortex 17:2491–2506.
Newman MEJ. 2004. Fast algorithm for detecting community structure in networks. Phys Rev E 69:066133. DOI: 10.1103/Physreve.69.066133.
Newman MEJ. 2006a. Finding community structure in networks using the eigenvectors of matrices. Phys Rev E 74:036104. DOI: 10.1103/Physreve.74.036104.
Newman MEJ. 2006b. Modularity and community structure in networks. Proc Natl Acad Sci U S A 103:8577–8582.
Newman MEJ, Girvan M. 2004. Finding and evaluating community structure in networks. Phys Rev E 69:026113. DOI: 10.1103/Physreve.69.026113.
Pardo JV, Lee JT, Sheikh SA, Surerus-Johnson C, Shah H, Munch KR, Carlis JV, Lewis SM, Kuskowski MA, Dysken MW. 2007. Where the brain grows old: decline in anterior cingulate and medial prefrontal function with normal aging. Neuroimage 35:1231–1237.
Peng D, Shi F, Shen T, Peng Z, Zhang C, Liu X, Qiu M, Liu J, Jiang K, Fang Y, Shen D. 2014. Altered brain network modules induce helplessness in major depressive disorder. J Affect Disord 168C:21–29.
Power JD, Cohen AL, Nelson SM, Wig GS, Barnes KA, Church JA, Vogel AC, Laumann TO, Miezin FM, Schlaggar BL, Petersen SE. 2011. Functional network organization of the human brain. Neuron 72:665–678.
Raz N, Lindenberger U, Rodrigue KM, Kennedy KM, Head D, Williamson A, Dahle C, Gerstorf D, Acker JD. 2005. Regional brain changes in aging healthy adults: general trends, individual differences and modifiers. Cereb Cortex 15:1676–1689.

Rubinov M, Sporns O. 2010. Complex network measures of brain connectivity: uses and interpretations. Neuroimage 52:1059–1069.

Rubinov M, Sporns O. 2011. Weight-conserving characterization of complex functional brain networks. Neuroimage 56:2068–2079.

Rypma B, Eldreth DA, Rebbechi D. 2007. Age-related differences in activation-performance relations in delayed-response tasks: a multiple component analysis. Cortex 43:65–76.

Saad ZS, Glen DR, Chen G, Beauchamp MS, Desai R, Cox RW. 2009. A new method for improving functional-to-structural MRI alignment using local Pearson correlation. Neuroimage 44:839–848.

Salthouse TA. 1991. Toward a General Theory of Expertise: Prospects and Limits. New York: Cambridge University Press.

Salthouse TA. 1996. The processing-speed theory of adult age differences in cognition. Psychol Rev 103:403–428.

Satterthwaite TD, Wolf DH, Loughead J, Ruparel K, Elliott MA, Hakonarson H, Gur RC, Gur RE. 2012. Impact of in-scanner head motion on multiple measures of functional connectivity: Relevance for studies of neurodevelopment in youth. Neuroimage 60:623–632.

Seghier ML. 2013. The angular gyrus: multiple functions and multiple subdivisions. Neuroscientist 19:43–61.

Seidler RD, Bernard JA, Burutolu TB, Fling BW, Gordon MT, Gwin JT, Kwak Y, Lipps DB. 2010. Motor control and aging: links to age-related brain structural, functional, and biochemical effects. Neurosci Biobehav Rev 34:721–733.

Smith SM, Jenkinson M, Woolrich MW, Beckmann CF, Behrens TEJ, Johansen-Berg H, Bannister, PR, De Luca M, Drobnjak I, Flitney DE, Niazy RK, Saunders J, Vickers J, Zhang YY, De Stefano N, Brady JM, Matthews PM. 2004. Advances in functional and structural MR image analysis and implementation as FSL. Neuroimage 23:S208–S219.

Song J, Desphande AS, Meier TB, Tudorascu DL, Vergun S, Nair VA, Biswal BB, Meyerand ME, Birn RM, Bellec P, Prabhakaran V. 2012. Age-related differences in test-retest reliability in resting-state brain functional connectivity. PLoS One 7:e49847.

Sorg C, Riedl V, Muhlau M, Calhoun VD, Eichele T, Laer L, Drzezga A, Forstl H, Kurz A, Zimmer C, Wohlschlager AM. 2007. Selective changes of resting-state networks in individuals at risk for Alzheimer's disease. Proc Natl Acad Sci U S A 104:18760–18765.

Sun Y, Danila B, Josic K, Bassler KE. 2009. Improved community structure detection using a modified fine-tuning strategy. Europhysics Letters 86:28004.

Szentagothai J. 1975. The 'module-concept' in cerebral cortex architecture. Brain Res 95:475–496.

Van Dijk KRA, Sabuncu MR, Buckner RL. 2012. The influence of head motion on intrinsic functional connectivity MRI. Neuroimage 59:431–438.

Xu CP, Zhang SW, Fang T, Ma MX, Qian CC, Chen HF, Zhu HW, Li YJ, Liu ZX. 2013. Altered functional connectivity within and between brain modules in absence epilepsy: a resting-state functional magnetic resonance imaging study. Biomed Res Int 2013:734893. DOI: 10.1155/2013/734893.

Address correspondence to:
*Mary E. Meyerand*
*Department of Biomedical Engineering*
*University of Wisconsin-Madison*
*1300 University Avenue*
*Madison, WI 53706*

*E-mail:* memeyerand@wisc.edu